

## COMPARATIVE ANALYSIS FOR LINK CROSS-SECTION OF MANIPULATOR ARMS

Dr. Ahmed Abdul Hussain Ali, Dler Obed Ramadhan  
Mech. Engr. Dept. /college of Engr. University of Baghdad

### ABSTRACT

The stresses and deflections in robot arm was analyzed using ANSYS software package. Industrial robot analyzed in this work consists of three arms that have 2-DOF. The analysis of each arm had been made separately.

The maximum stress and deflection have been analyzed for a static applied at one end of the arm while has the other end fixed. Links of various cross-sections having same masses, length, and material properties to make a choice of the shape that gives a high stiffness to weight ratio have been examined. After specifying the best section for the arms of the robot an optimization process began to determine the dimensions of the arms sections which give the least deformation this had been done by the aid of a program build up by using the MATHCAD software package. In the beginning the program finds the optimum section in which the stress in the members not exceeds the allowable stress and finds the total weight of the robot after that the program begins to change the dimensions to satisfy the condition of minimum deflection of the whole robot after that the program estimates the best choices of the dimension for each section that gives the minimum weight and deflection.

The dynamic behavior of the best chosen structure of industrial robot was studied to find the natural frequencies ( $w_n$ ) and mode shapes.

The result shows that the hollow circular section is the best section for the first link while a square section is the best section for the other two links.

### الخلاصة

تم استخدام طريقة العناصر المحددة في هذا البحث بالاستعانة ببرنامج (ANSYS) لتحليل الاجهادات والتشوهات في ذراع الروبوت, حيث تم تحليل ودراسة روبوت مكوّن من ثلاثة اذرع ذا درجتين من الحرية, وتم تحليل كل ذراع على الانفراد. تمت دراسة الاجهادات والتشوهات العظمى نتيجة القوى الساكنة المؤثرة على الطرف الحر للذراع, حيث تم اختيار مقاطع مختلفة لاذرع الروبوت والتي لها نفس الكتلة والطول والمعدن لاجل اختيار افضل مقطع والذي يعطي نسبة متانة الى وزن عالية. وبعد ان تم تحديد افضل مقطع لذراع الروبوت قمنا باجراء عملية الامثلية (OPTIMIZATION) لاجل تحديد ابعاد المقطع الذي يعطي اقل تشوه حيث تم الاستعانة ببرنامج مكتوب بواسطة ال (MATHCAD).

البرنامج في البداية حدد المقطع الامثل الذي يكون فيه الاجهاد اقل من الحد الاقصى المسموح به وبعدها تم ايجاد وزن هيكل الروبوت ومن ثم يقوم البرنامج بتغيير الابعاد لاجل تقليل التشوه الكلي عند نهاية ذراع الروبوت حيث تم تحديد ابعاد افضل مقطع يملك اقل وزن وتشوه.

كما وتم دراسة السلوك الديناميكي للهيكال الامثل وتحديد شكل الاطوار والترددات الرنينية. النتائج بينت بأن افضل مقطع للذراع الاول العمودي هو المقطع الدائري المجوف اما الذراع الثاني والثالث فالافضل هو المقطع المربع المجوف.

**KEYWORDS:** Manipulator design, Structural stiffness, Robotics, Robot design, Optimization, Comparative structural analysis, Finite-element analysis, Structural optimization

## INTRODUCTION

Industrial manipulators usually consist of a rigid kinematics chain built up of several rigid links which are connected by direct driven linear or rotational joints in order to move high payloads with high speed and high position accuracy. The slackness in the gears as well as the deformations in the links, which occurs under load, must be eliminated. This can only be reached using rigid joint actuators and rigid links resulting in heavy structure.

Rigid link manipulators require height stiff structures to achieve high accuracy and low inertias.

General handbooks to aid in the design of manipulator exist in literature (**Rivin 1988&Shimon1999**). Analysis of stiffness of manipulator links can be found in (**Rivin 1988**) and (**Leu et al. 1985**), optimization techniques and calibration techniques have been used to correct errors in accuracy.

Robot designers have attempted to systematically develop analytical criteria for the design of critical components. For example (**Fresonke et al. 1993**) has set analytical criteria for the deflection prediction of serial manipulators. (**Henessey et al. 2000**) has demonstrated the design of a light weight manipulator arm while (**Williams et al.1993**), has demonstrated the design of an isotropic six-axis manipulator arm. (**Rivin 1988**) has compared a variety of structural material used in manipulator arms and has studied critical design components. Fault-tolerant method for manipulator-joint development was introduced by (**Wu et al. 1993**), while the design of fault tolerant manipulators was addressed by (**Paredis 1996**).

Prismatic joints of manipulator arms based upon across sectional design of the links that provides a high stiffness to weight ratio compared with a hollow round cross-section has been addressed by (**Abdelmalek 1998**).

(**Alazard, 1992**) describe three different techniques to build up the dynamic model of SECAFLEX, a 2-DOF flexible in plane manipulator driven by geared Dc motors, they study the effect of angular configuration changes and physical parameters modifications and shows that the three techniques give similar result up to the first flexible modes of each link when concentrated masses and inertias are present.

(**Shiakolas et al. 2002**) discussed optimum robot design based on task specifications using evolutionary optimization approaches, these approaches were used for the optimum design of SCARA and articulated 3-DOF PUMA type manipulators.

The process of optimal design of robots having stochastic model parameters (e.g. material, geometry or load) had been viewed by (**Haubach 2002**) as a stochastic structural task, using flexible structures; the goal is the minimization of the total weight of the robot under certain constraints concerning the deviation between the actual and the prescribed path in workspace.

The work of (**Marcus et al. 2004**) presents an optimization procedure which shows how optimization can be used in the early phases of a development process in order to evaluate the potential of a concept. The objective in the optimization is to determine optimal gearboxes and arm lengths from an acceleration capability perspective. The arm lengths are treated as continuous variables where as the gearbox are selected from a list of available units. The object of their work is a 3-DOF robot modeled in the mathematics program and optimized using the complex optimization algorithm.

In this work a comparison had been made between five candidate sections (square, circular, two vertically tube, two horizontally tube and tri tube) to chose the best section for constructing a three arm robot manipulator that has 2-DOF. Analysis had been done by using ANSYS software package and its results are compared with those obtained by the traditional ways used in strength of materials and by the aid of MATHCAD software. An optimization problem for the dimensions of

the cross section had been analyzed to get the best construction that has the minimum weight and with stand the given payload and gives a minimum deflection.

### PROBLEM DEFINITION

When a robot is assigned to carry a payload, certain stress distribution develops along the arm. The characteristics of this stress depend on the material, the geometrical design of the robot arm and other external factors such as the interaction of the robot with the environment. It is necessary to know what the most critical configuration is in order to optimize the robot design. Although it depends on the overall kinematics' design of each robot in general this position corresponds to the configuration where the arm is fully extended so that the moment arm is maximized.

### DESIGN THEORY

The types of stresses subjected on the robot arm are bending (neither shear nor torsion). So a good criteria evaluator (for general and particular cases) that compiles them is the Von Misses theory. The Von Misses failure criterion is a theory based on the distortion energy in a given material; it is the energy associated with changes in the shape of the material. A given component is safe as long as the maximum value of the distortion energy per unit of volume in the assigned material remains smaller that the distortion energy per unit volume required causing yield in a tensile-test specimen of the same material. This theory later will be used to secure that no failure will occur in any of the arms (links).

Most manipulator link cross-sections are hollow. Hollow links provide convenient conduits for electric power and communication cables, hoses, power transmission members, etc.

In this research a different hollow cross-section is introduced, consisting of square, three tubes centered on the vertices of an equilateral triangle (this cross section is referred to as a tri-tube configuration), two horizontally tubes (this cross section is referred to as a 2H-tubes configuration), cylindrical link (will be referred to as a uni-tube configuration), and two vertically tubes (this cross section is referred to as a 2V-tubes configuration). As shown in **Fig. (1)**

Links with an open end manipulator are normally modeled as cantilevers .As shown in **Fig. (2)**.

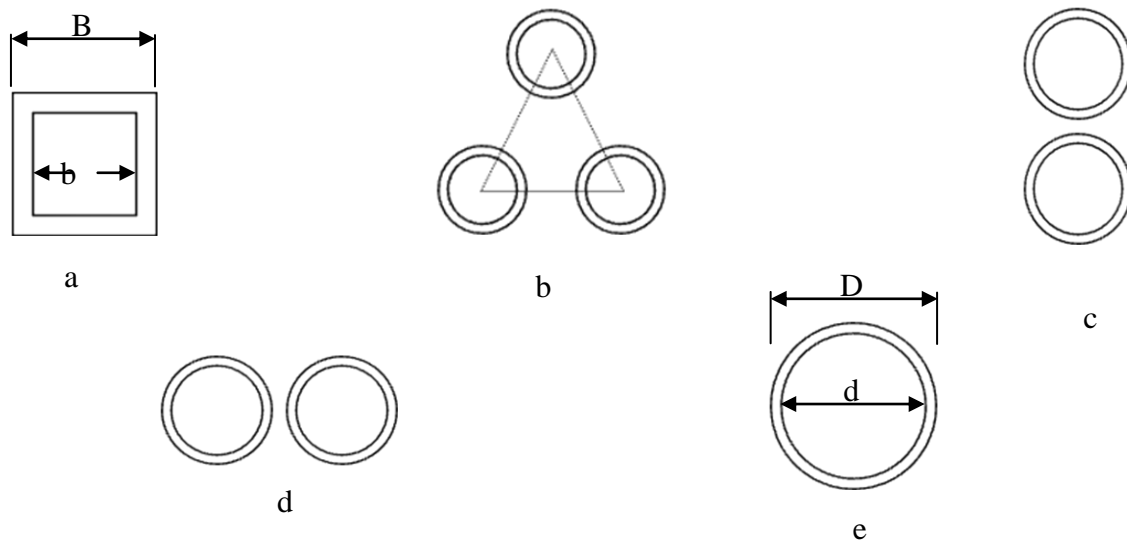
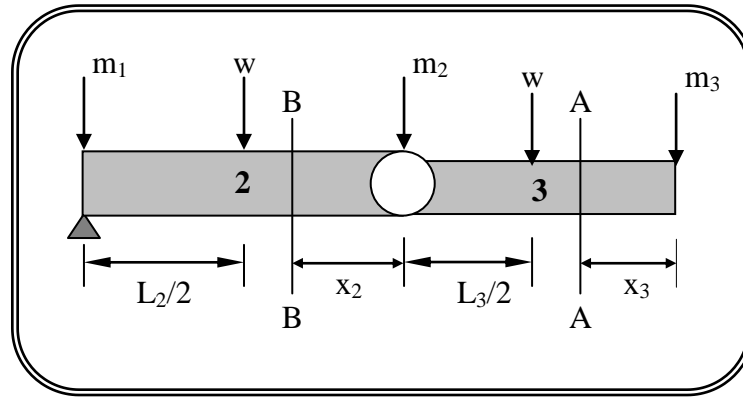


**Fig. (1) Type of sections studied**

**(a) Square Cross-Section, (b) Tri-Tube Cross-Section, (c) Two Vertically-Tube Cross-Section, (d) Two Horizontally-Tube Cross-Section, (e) Uni-Tube Cross-Section**



Fig(2) Forces on Modeled Arm

$$M_{A-A} = m_3 g x + q_3 \frac{x^2}{2} \quad (1)$$

Where:

$M_{A-A}$  = Bending moment at the third arm

$m_3$  = Payload =10kg

$g$  = Specific gravity

$q_3$  = Weight per unit length of third arm

When  $x=L$  bending moment is maximum [8]

$$M_{A-A} \Big|_{\max} = m_3 g L_3 + q_3 \frac{L_3^2}{2} \quad (2)$$

$$\sigma_3 = \frac{M Y}{I} \quad (3)$$

Where:

$\sigma_3$  = Bending stress at the third arm

$I$  = Second moment of the cross-sectional area

$Y$  = Centroid-moment of the cross area

Substituting equation (2) into (3) gives the equation below:

$$\sigma_3 = \frac{\left( m_3 g L_3 + q_3 \frac{L_3^2}{2} \right) Y}{I} \quad (4)$$

$$\delta y_3 = \frac{W L^3}{3E I} + \frac{w L^4}{8E I} \quad (5)$$

$$= \left( \frac{m_3 g L_3^3}{2} + \frac{q_3 L_3^4}{8} \right) \frac{1}{E I} \quad (6)$$

$$q_3 = \gamma A = \rho g A \quad (7)$$

Where:

$\delta y_3$  = Deflection at the third arm.

$E$  = Modulus of elasticity.

$\rho$  = Density of material.



$$q_3 = 7850 * 9.81 * A \quad (8)$$

$$M_{B-B} = m_2 g x_2 + q_2 \frac{x_2^2}{2} + q_3 L_3 \left( \frac{L_3}{2} + x_2 \right) + m_3 g (L_3 + x_2) \quad (9)$$

Where [8]:

$M_{B-B}$  = Bending moment at the second arm

$m_2$  = Mass of the second arm

When  $x_2=L_2$  bending moment is maximum

$$M_{B-B})_{\max} = m_2 g L_2 + q_2 \frac{L_2^2}{2} + q_3 L_3 \left( \frac{L_3}{2} + L_2 \right) + m_3 g (L_3 + L_2) \quad (10)$$

$$\sigma_2 = \frac{M Y}{I} \quad (11)$$

$$\sigma_2 = \frac{\left( m_2 g L_2 + q_2 \frac{L_2^2}{2} + q_3 L_3 \left( \frac{L_3}{2} + L_2 \right) + m_3 g (L_3 + L_2) \right) Y}{I} \quad (12)$$

Where:

$\sigma_2$  = Bending stress at the second arm

$$\delta y_2 = \frac{W L^3}{3E I} + \frac{w L^4}{8E I} + \frac{M L^2}{2E I} \quad (13)$$

$$= \frac{1}{E I} * \left( \frac{\left( (m_2 + m_3) g + q_3 L_3 \right) L_2^3}{3} + \frac{q_2 L_2^4}{8} + \frac{\left( \left( m_3 g L_3 + q_3 \frac{L_3^2}{2} \right) L_2^2 \right)}{2} \right) \quad (14)$$

$$W_{Total} = g (m_1 + m_2 + m_3) + q_3 L_3 + q_2 L_2 \quad (15)$$

$$M_{Total} = q_3 \left( L_3 L_2 + \frac{L_3^2}{2} \right) + q_2 \frac{L_2^2}{2} + m_3 g (L_3 + L_2) + m_2 g L_2 \quad (16)$$

$$\sigma_{bending} = \frac{M_{Total} * Y}{I} \quad (17)$$

$$P_{cr})_{strut} = \frac{\pi^2 E I}{4L^2} \quad (18)$$

Where:

$P_{cr}$  = Critical load.

$$\sigma_{strut} = \frac{P_{cr}}{A} \quad (19)$$

$$\sigma_1 = \sigma_{strut} + \sigma_{bending} \quad (20)$$

Where:

$\sigma_1$  = Combined stress at the first arm.

$\sigma_{strut}$  = Strut stress.

$$\frac{1}{\sigma_r A} = \frac{1}{\sigma_e A} + \frac{1}{\sigma_c A}$$

From this equation we see that:

$$\begin{aligned} \frac{1}{\sigma_r A} &= \frac{1}{\sigma_e A} + \frac{1}{\sigma_c A} \Rightarrow \frac{1}{\sigma_r} = \frac{1}{\sigma_e} + \frac{1}{\sigma_c} = \frac{\sigma_e + \sigma_c}{\sigma_e \sigma_c} \\ \sigma_r &= \frac{\sigma_c}{1 + \frac{\sigma_c}{\sigma_e}} \end{aligned} \quad (21)$$

Where:

$\sigma_r$  : Rankine stress

$\sigma_e$  : Euler stress

For a strut with one end fixed, the other free

$$\sigma_e = \frac{\pi^2 E I}{4 L^2 A} \quad (22)$$

$$I = A k^2 \Rightarrow k = \sqrt{\frac{I}{A}} = \sqrt{\frac{\frac{\pi}{64} (D_1^4 - d_1^4)}{\frac{\pi}{4} (D_1^2 - d_1^2)}} \quad (\text{For uni-tube section})$$

$$\Rightarrow k = \frac{1}{4} \sqrt{(D_1^2 + d_1^2)}$$

$$\sigma_e = \frac{\pi^2 E k^2}{4 L^2} = \frac{\pi^2 E}{4 \left(\frac{L}{k}\right)^2} \quad (23)$$

Substituting equation (23) into equation (21) yields (**Hearn 1977**):

$$\sigma_r = \frac{\sigma_c}{1 + \frac{\sigma_c}{\pi^2 E} 4 \left(\frac{L}{k}\right)^2} \quad (24)$$

For comparing between the sections the weight of the gears and gripper were neglected the parameter of each arm as bellow:

$$L_1=0.3\text{m}, L_2=0.2\text{m}, L_3=0.15\text{m}$$

$$m_1=8.8781\text{kg}, m_2=1.9691\text{kg}, m_3=1.278\text{kg}$$

Where:

$m_1, m_2, m_3$ = the mass of first, second and third arm, respectively

$$E= 200 \cdot 10^9 \text{ N/m}^2, \nu = 0.3$$

$$g= 9.81$$

$$\text{Payload}= 100\text{N}$$

### Deflections Due to Pure Bending

The deflection  $\delta$  is evaluated using finite element analysis techniques when the manipulator is at its maximum reach (completely stretched out) since this will yield the maximum deflection. Any other configuration will yield a smaller deflection value considering that the same

payload is carried. The deflection evaluation is a function of the structural and material properties of the links and the payload.

- **Square Cross-Section**

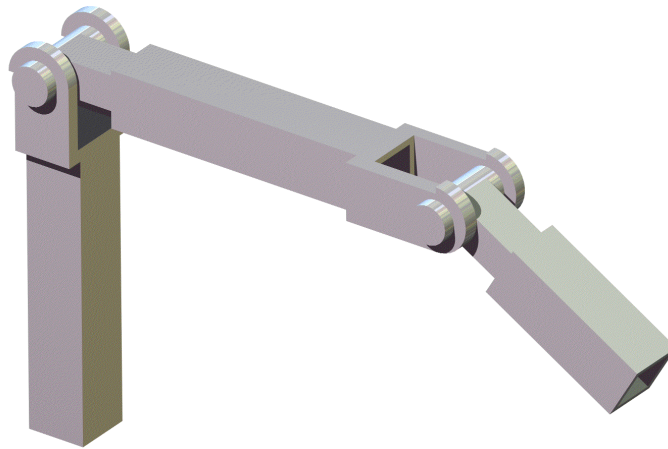


**Fig. (3) Robotic Arm of Square Cross-Section**

The cross-sectional parameters for each arm of the square section are given in **Table (1)**:

**Table (1a) Model Parameters for First Arm Square Cross-Section**

$B_1$ (m)	0.064	0.071	0.078	0.085	0.092
$b_1$ (m)	0.018	0.036	0.048	0.059	0.069

**Table (1b) Model Parameters for Second Arm Square Cross-Section**

$B_2$ (m)	0.04	0.047	0.054	0.061	0.068	0.075
$b_2$ (m)	0.0187	0.0309	0.0408	0.0497	0.0580	0.0661

**Table (1c) Model Parameters for Third Arm Square Cross-Section**

$B_3$ (m)	0.035	0.042	0.049	0.056	0.063	0.07
$b_3$ (m)	0.012	0.0261	0.0363	0.0453	0.0537	0.0618

- **Tri-Tube Cross-Section**

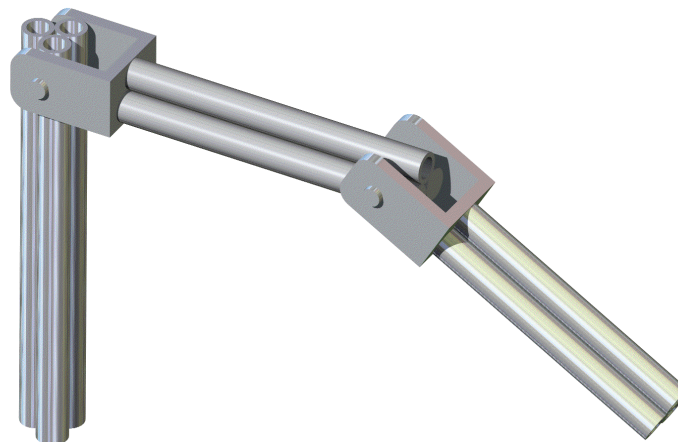


**Fig. (4) Robotic Arm of Tri-Tube Cross-Section**

The cross-sectional parameters for each arm are given in **Table (2)**:

**Table (2a) Model Parameters for First Arm Tri-Tube Cross-Section**

D <sub>1</sub> (m)	0.0425	0.0495	0.0565	0.0635	0.0705
d <sub>1</sub> (m)	0.0251	0.0357	0.0449	0.0534	0.0616

**Table (2b) Model Parameters for Second Arm Tri-Tube Cross-Section**

D <sub>2</sub> (m)	0.03	0.037	0.044	0.051	0.058
d <sub>2</sub> (m)	0.02465	0.03281	0.04054	0.04804	0.05542

**Table (2c) Model Parameters for Third Arm Tri-Tube Cross-Section**

D <sub>3</sub> (m)	0.0179	0.0249	0.0319	0.0389
d <sub>3</sub> (m)	0.00141	0.01736	0.02644	0.03456

- **Two Horizontally-Tube Cross-Section**

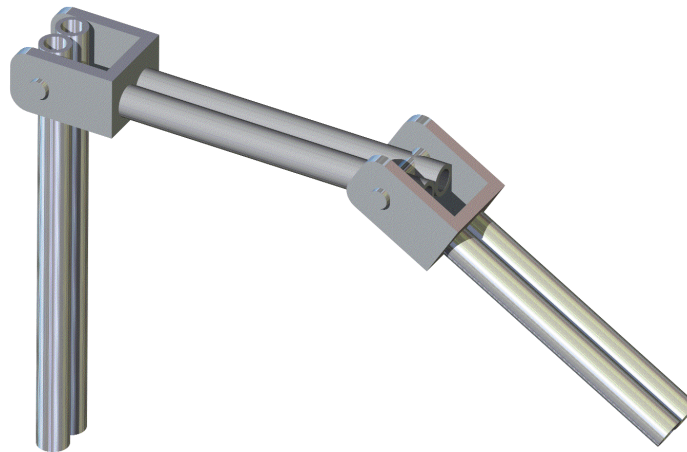


**Fig. (4) Robotic Arm of 2H-Tube Cross-Section**

The cross-sectional parameters for each arm are given in **Table (3)**:

**Table (3a) Model Parameters for First Arm 2H-Tube Cross-Section**

D <sub>1</sub> (m)	0.05	0.057	0.064	0.071	0.078
d <sub>1</sub> (m)	0.0279	0.0391	0.0487	0.0576	0.066

**Table (3b) Model Parameters for Second Arm 2H-Tube Cross-Section**

D <sub>2</sub> (m)	0.04	0.047	0.054	0.061	0.068
d <sub>2</sub> (m)	0.0362	0.04383	0.05127	0.05859	0.06585

**Table (3c) Model Parameters for Third Arm 2H-Tube Cross-Section**

D <sub>3</sub> (m)	0.02	0.027	0.034	0.041	0.048
d <sub>3</sub> (m)	0.0079	0.0197	0.0286	0.0366	0.04434



**Uni-Tube Cross-Section**

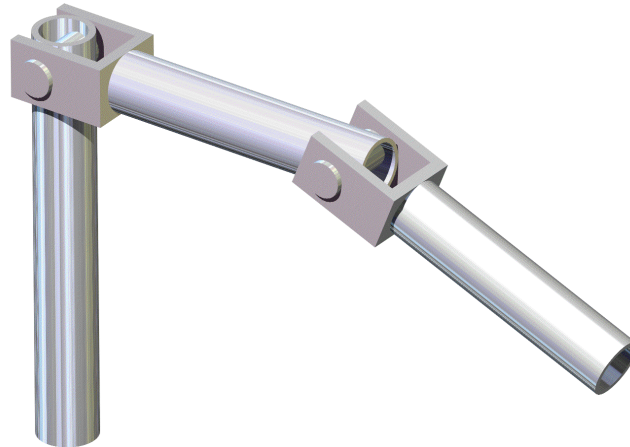


**Fig. (6) Robotic Arm of Uni-Tube Cross-Section**

The cross-sectional parameters for each arm are given in **Table (4)**:

**Table (4a) Model Parameters for First Arm Uni-Tube Cross-Section**

$D_1(m)$	0.07	0.077	0.084	0.091	0.098	0.105	0.112	0.119	0.126
$d_1(m)$	0.01	0.034	0.047	0.059	0.0693	0.079	0.088	0.097	0.105

**Table (4b) Model Parameters for Second Arm Uni-Tube Cross-Section**

$D_2(m)$	0.05	0.057	0.064	0.071	0.078	0.085
$d_2(m)$	0.03	0.0406	0.05	0.0586	0.067	0.075

**Table (4c) Model Parameters for Third Arm Uni-Tube Cross-Section**

$D_3(m)$	0.04	0.047	0.054	0.061	0.068	0.075
$d_3(m)$	0.015	0.0288	0.0392	0.0484	0.057	0.0651

- Two Vertically -Tube Cross-Section**

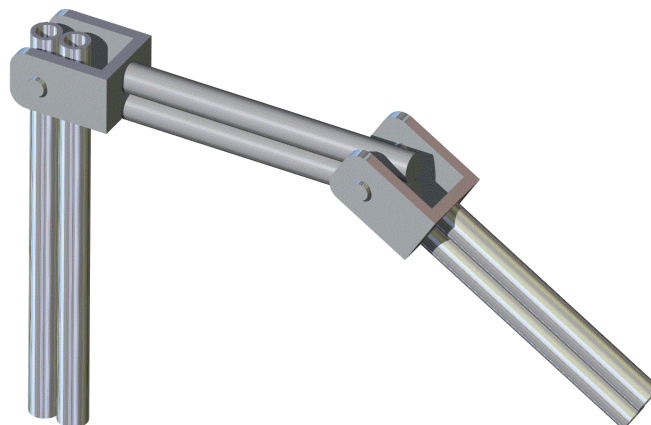


**Fig. (7) Robotic Arm of 2V-Tube Cross-Section**

The cross-sectional parameters for each arm are given in **Table (5)**:

**Table (5a) Model Parameters for First Arm 2V-Tube Cross-Section**

D <sub>1</sub> (m)	0.05	0.057	0.064	0.071	0.078
d <sub>1</sub> (m)	0.0279	0.0391	0.0487	0.0576	0.066

**Table (5b) Model Parameters for Second Arm 2V-Tube Cross-Section**

D <sub>2</sub> (m)	0.04	0.047	0.054	0.061	0.068
d <sub>2</sub> (m)	0.0362	0.04383	0.05127	0.05859	0.06585

**Table (5c) Model Parameters for Third Arm 2V-Tube Cross-Section**

D <sub>3</sub> (m)	0.02	0.027	0.034	0.041	0.048
d <sub>3</sub> (m)	0.0079	0.0197	0.0286	0.0366	0.04434

## OPTIMIZATION OF THE ROBOT STRUCTURE

Our overall goal is to design a robot arm that is stiff, lightweight, and exhibits minimum number of low natural frequencies for rigid-body structural dynamics (i.e., structural resonances). It is well known that, when a structure design is optimized to achieve high fundamental vibration frequencies, it also achieves the concomitant goal of low mass. Our initial design suggested that an arm design possessing high structural vibration frequencies while carrying a gripper payload, typically also satisfies the otherwise contradictory objectives of low mass, high stiffness, and high strength.

The objective function of these problems was to minimize the weight of the structures, subject to constraints on the stress in the robotic arm and displacement constraints at the end effectors. The design variables were the cross sectional shape of the robotic arm.

There are two cases of optimization in this research. The first case, which referred to as initial optimization, was to optimize the cross-sectional shape, and the second case, that referred to as final optimization, was to apply the optimization techniques to an actual structure.

### Initial Optimization:

### Optimization Invariants:

The following parameters shown in **Table (6)** are invariant over all five cross-sectional:

**Table (6) Invariant Parameters**

Structural Characteristics	First Arm	Second Arm	Third Arm
L	0.3m	0.2m	0.15m
Material	Steel	steel	steel
E	200*10 <sup>9</sup> N/m <sup>2</sup>	200*10 <sup>9</sup> N/m <sup>2</sup>	200*10 <sup>9</sup> N/m <sup>2</sup>
$\rho$	7850 kg/m <sup>3</sup>	7850 kg/m <sup>3</sup>	7850 kg/m <sup>3</sup>
$\nu$	0.3	0.3	0.3
A	3.77*10 <sup>-3</sup> m <sup>2</sup>	1.25*10 <sup>-3</sup> m <sup>2</sup>	1.08*10 <sup>-3</sup> m <sup>2</sup>
Mass of arm	8.8781kg	1.9691kg	1.278kg



**Optimization Variables:**

The following variables were optimized for each link to achieve the highest stiffness and minimum deflection for the overall structure of the industrial robot:

- Shape of the arm cross-section.
- Moment of inertia for each arm.

**Final Optimization:**

**Optimization Invariants:**

The parameters shown in **Table (7)** are invariant over all five cross-sectional:

**Table (7) Invariant Parameters**

Structural Characteristics	First Arm	Second Arm	Third Arm
L	0.3m	0.2m	0.15m
Material	Steel	steel	steel
E	200*10 <sup>9</sup> N/m <sup>2</sup>	200*10 <sup>9</sup> N/m <sup>2</sup>	200*10 <sup>9</sup> N/m <sup>2</sup>
ρ	7850 kg/m <sup>3</sup>	7850 kg/m <sup>3</sup>	7850 kg/m <sup>3</sup>
ν	0.3	0.3	0.3
T	0.002m	0.002m	0.002m
Mass of gears	15kg	15kg	30kg
Cross-section	Hollow circular	Hollow square	Hollow square

**Optimization Variables:**

The following variables were optimized for each link to achieve the highest stiffness, and minimum deflection for the overall structure of the industrial robot:

- Inner diameter for the first circular tube arm.
- The inner side dimension for the second and third square tube arm.
- Total mass of industrial robot.
- Natural frequencies ( $w_n$ ) and mode shapes.

Reducing the weight or changing the shape of a robot is not an easy task to accomplish; there are several factors involved in this, such as the type of external load that the manipulator is subjected to, material used (links of the robot) and the most complex variable to handle is its shape (geometry). The complexity introduced by these factors make it awkward to calculate the stress levels by hand. For this reason, an FEA package is needed; in this particular case ANSYS is used. This software will calculate how the von Misses stress is distributed along the links. Results are compared to the permissible or yield stresses, which make it possible to know if any arm is under failure mode.

$$\sigma (\text{Von Misses Stress}) \leq \sigma_y (\text{Yield Strength}).$$

To accomplish the goal of reducing the weight of the structure; therefore, improving its performance and the payload capacity, the weight distribution of the whole structure should be revised. Every link needs to be taken into account in order to avoid high inertial loads and an unstable robot design. A robotic design should follow the rule that the first link should be the most robust and the outermost as light as possible (The first link is going to hold the weight of the whole structure plus the payload).

## RESULTS AND DISCUSSION

In this work we chose five types of tube sections (square, circular, two vertical, two horizontal and three circular) to make a comparison between them and to choose the best section for constructing a three arm robot manipulator.

The procedure of analysis is based on assigning a certain mass and length for each of the first, second and third arm of the manipulator after that we calculate the cross sectional area for each arm and then we assume a certain dimension like the outer diameter of the circular tube and calculating the corresponding inner diameter after that we change the outer diameter by increasing it by a specific amount. The same procedure is used for all sections except for the 2V-tube, 2H-tube and tri-tube sections where the mass of the stiffeners must be subtracted from each arm before calculating the cross sectional area of each arm. After these initial calculations and after estimating the dimensions of each section we begin entering these data to the ANSYS software program to calculate the deformations and stress for each arm those results are shown in **Figures (8-13)** which demonstrates the regions where maximum stress and deformations occurs. The results for maximum deflections and those for maximum stresses for each arm and different cross sections are all collected from which we plot the figures and make the conclusions that for the first arm of the robot manipulator it is best to make its section as a circular tube this conclusion is clear from **Figure (14)** where for a given maximum stress the stiffness for the circular section is bigger as compared with the other sections this result is also clear in **Figure (15)** for a given maximum stress the uni-tube gives less deformation from other sections.

For the second arm we make a conclusion that the square section has a low stress for a given stiffness this is clear in **Figure (16)** and also in **Figure (17)** for a given deflection the stress will be minimum in the square section.

The same results is obvious in **Figure (18)** where for a given deflection the stress is minimum for the square section the same conclusion is clear in **Figure (19)** where for a given stiffness the stress is minimum in the square section, the same result may be achieved from **Figure (20)** where for a given moment of inertia the square section gives higher stiffness relative to the other sections.

To make a self checking for our results in ANSYS, a program had been built up using MATHCAD software. The results of calculation by MATHCAD are shown in **Figures (21-26)** where the same conclusion are drawn up from the curves that is the first arm of the robot manipulator is preferred to make its section as a circular tube while the other two arms it is preferred to make its section as a square tube to achieve higher stiffness to weight ratio. In this calculations the same dimensions of each section of each arm had been given as an input data for the program so as to make the comparison between the two ways of analysis essayer, the differences between the results is referred to the way of analysis in each software, where in ANSYS the analysis is based on finite element and in MATHCAD the analysis is based on the solution on the known equations of strength of materials for finding the maximum stress and deflections in beams and struts, due to those different ways of analysis a slight error is seen in those figures, such error don't play a big rule from the engineering point of view.

The next step in our work was to built another program to make an optimum design for a given robot having a given length of arms and payload and to find the best dimensions for its first, second and third arm.

The program had been written by MATHCAD software and it begins as assigning the length of the three arms and the mass of the first and second gear box actuator and the total mass of the payload, that the robot (manipulate), and its end effector actuator.

The sequence of calculations begins by finding the dimensions of the arm cross section that satisfies the condition of strength that is to let the stress in each arm be the maximum possible value it can reach, after that the program find the weight of the arms of the robot. The next step in this program is to change the dimension step by step to make the structure of the robot stiffer, the

iteration continuous until the program fined the dimension of each section that satisfies the limits of deflection on the end point of the robot arm that we want the robot to achieve in the same time the program makes checking on the weight of robot structure if it is higher than the limit that it is assigned to it. From all those iterations and results that the program reaches (which satisfy the conditions of weight and deflection) it chooses the best design parameter between all the result that has the less weight and deflection due to the given condition of loading.

The final dimension of the robot arms will be the next input for the ANSYS to calculate the dynamic characteristics of the structure of the robot to determine its natural frequency and mode shapes of vibration.

The iterations shows that if we increase the weight of the robot by about 25% of the initial weight calculated in our first analysis, in which ( $\sigma \leq \sigma_y$  in each arm), the iteration gives us 32 generation which satisfies our condition of deflection ( $0.005m < \delta_{max} < 0.002m$ ) those results for the dimensions of the inner diameter of the first arm and the inner side dimension of the second and third arm are show in **Figure (27)**.

A plot of the total deformation of the end effectors is shown in **Figure (28)** for each generation. **Figure (29)** shows the total weight of the robot structure for each generation.

The criteria for choosing the best dimensions for the robot structure from the 32 generation obtained is to multiply the weight of each generation by it's deflection the result of multiplication gives us an indication of the best generation which has the less value between them, and this criteria is referred to as the criteria of choice, which is shown in **Figure (30)** it is obvious that the 21 generation in the best between them the dimension of this generation entered to ANSYS to calculate the natural frequencies and mode shapes for the robot structure. The results of dynamic analysis show that the natural frequencies are (53.614, 59.171, and 138.70Hz). **Figure (31-33)** shows the mode shapes for each natural frequency calculated.

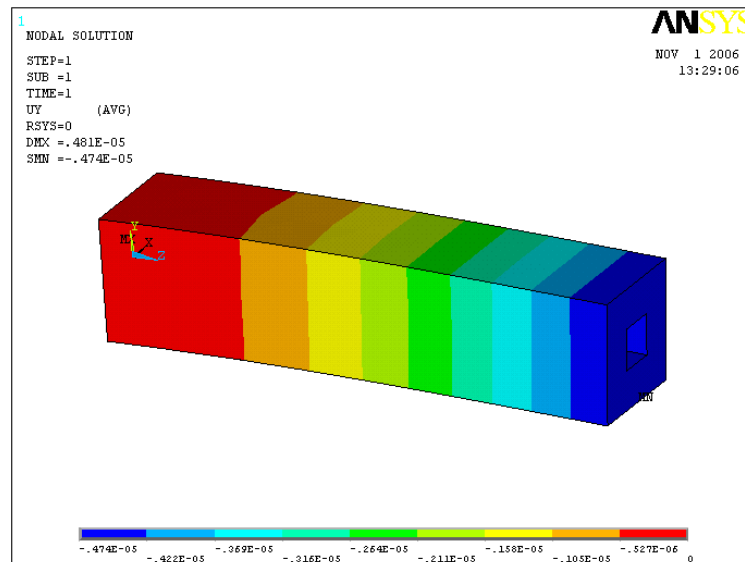


**Fig. (8) Deflection in the Third Arm of Square Cross-Section where  $B=0.035m$ ,  $b=0.012m$**

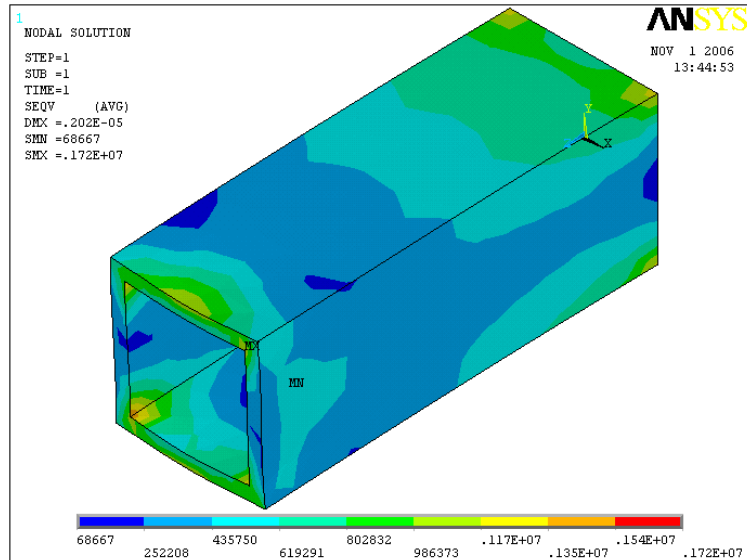


Fig. (9) Stress in the Third Arm of Square Cross-Section where  $B=0.056m$ ,  $b=0.0453m$

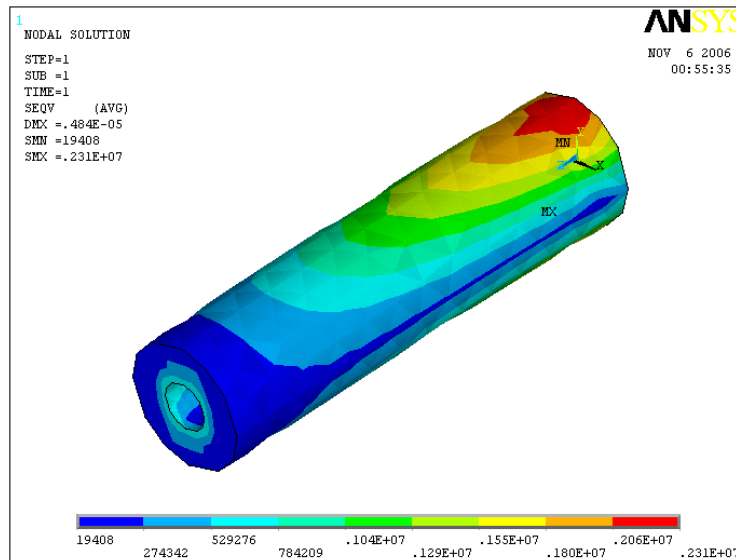


Fig. (10) Stress in the Third Arm of Uni-Tube Cross-Section where  $D=0.04m$ ,  $d=0.015m$

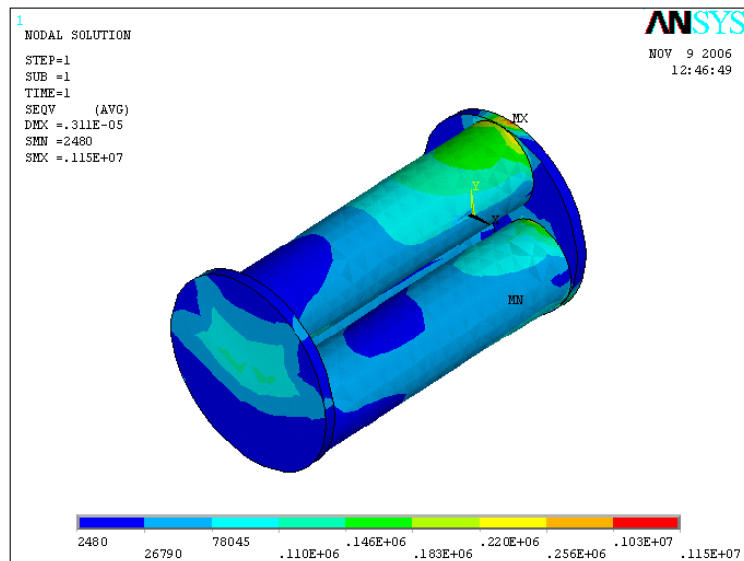


Fig. (11) Stress in the Third Arm of Tri-Tube Cross-Section where  $D=0.0389m$ ,  $d=0.03456m$

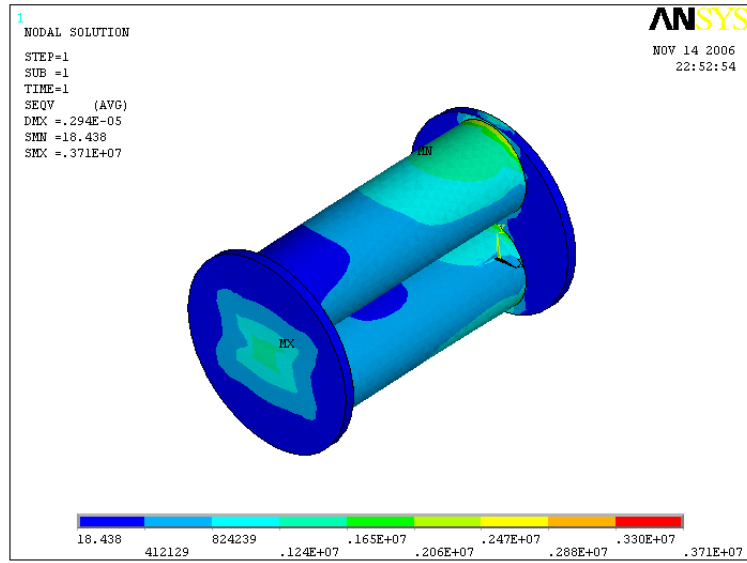


Fig. (12) Stress in the Third Arm of 2V-Tube Cross-Section where  $D=0.048m$ ,  $d=0.04434m$

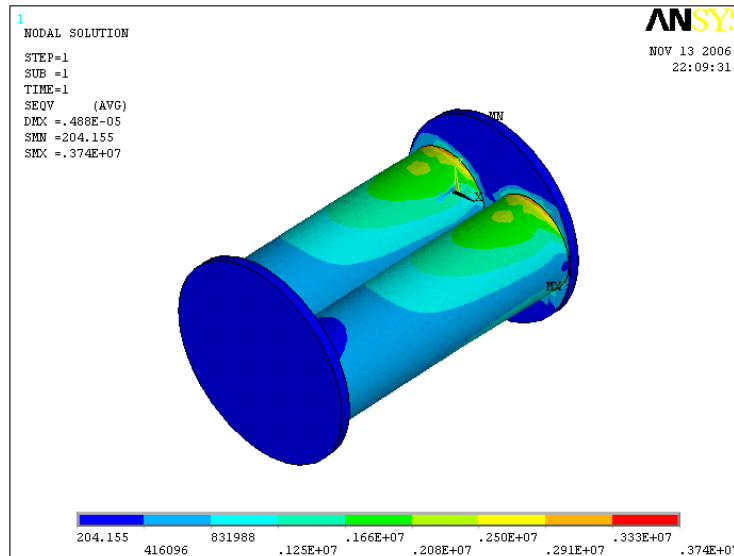


Fig. (13) Stress in the Third Arm of 2H-Tube Cross-Section where  $D=0.048m$ ,  $d=0.04434m$

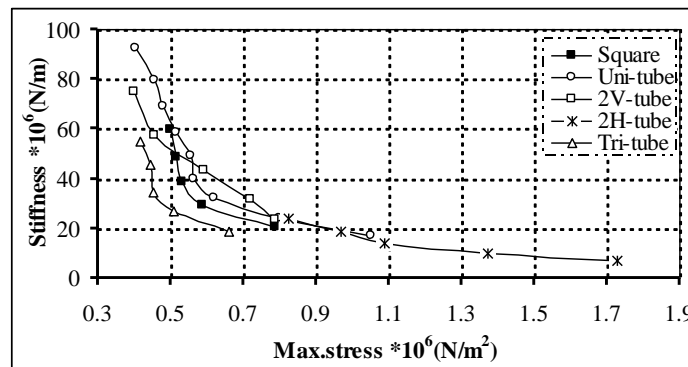


Fig. (14) Stiffness Versus Maximum Stress in the First Arm for Different Cross-Sections by ANSYS

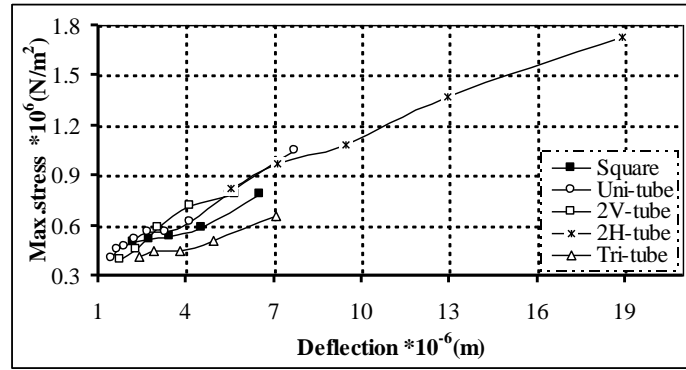


Fig. (15) Maximum Stress Versus Deflection in the First Arm for Different Cross-Sections by ANSYS

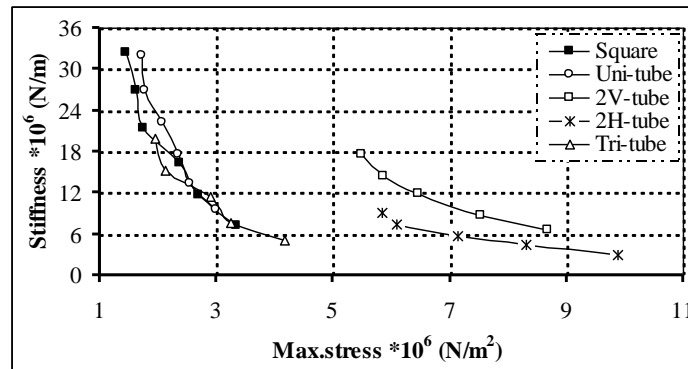


Fig. (16) Stiffness Versus Maximum Stress in the Second Arm for Different Cross-Sections by ANSYS

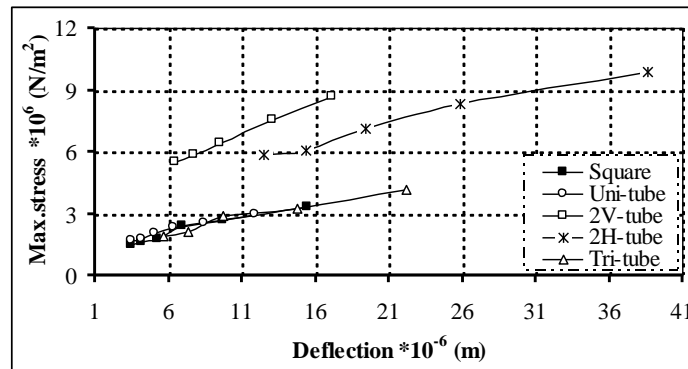


Fig. (17) Maximum Stress Versus Deflection in the Second Arm for Different Cross-Sections by ANSYS



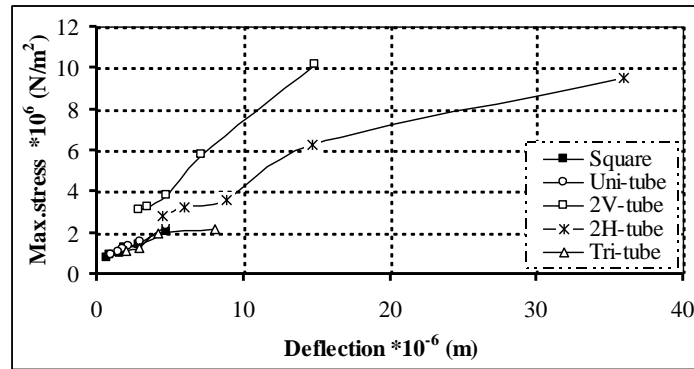


Fig. (18) Maximum Stress Versus Deflection in the Third Arm for Different Cross- Sections by ANSYS

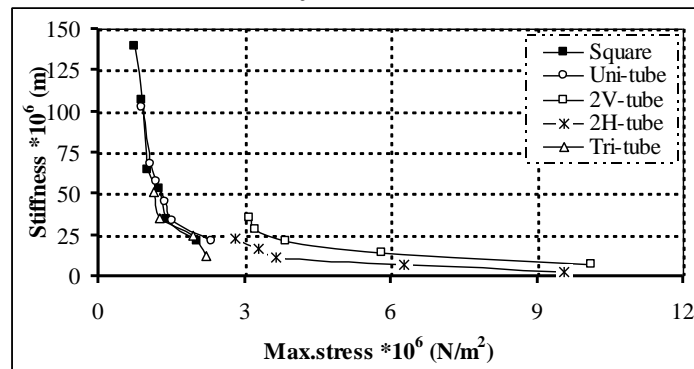


Fig. (19) Stiffness Versus Maximum Stress in the Third Arm for Different Cross-Sections by ANSYS

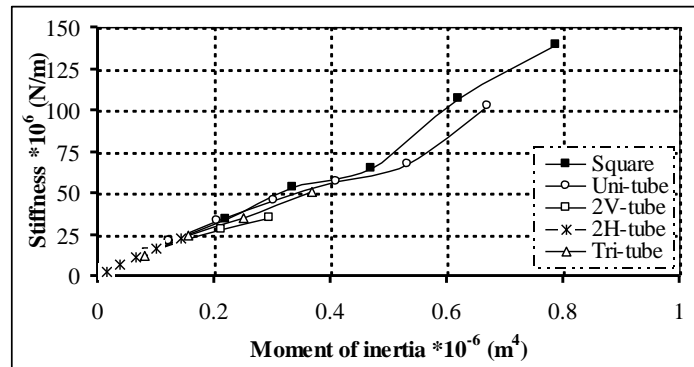


Fig. (20) Stiffness Versus Moment of Inertia in the Third Arm for Different Cross-Sections by ANSYS

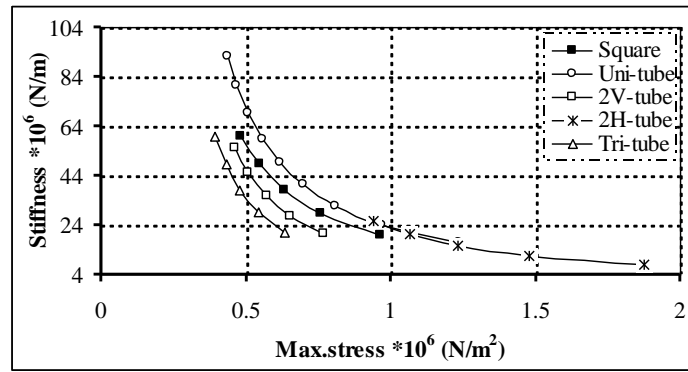


Fig. (21) Stiffness Versus Maximum Stress in the First Arm for Different Cross-Sections by MATHCAD

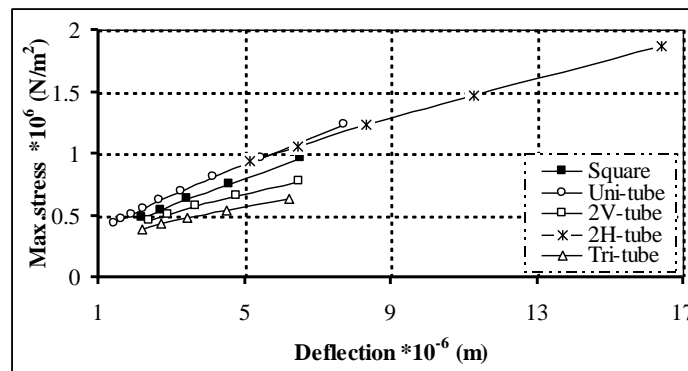


Fig. (22) Maximum Stress Versus Deflection in the First Arm for Different Cross-Sections by MATHCAD

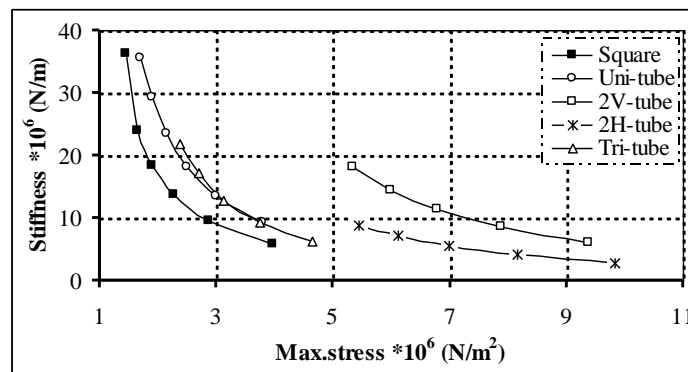


Fig. (23) Stiffness Versus Maximum Stress in the Second Arm for Different Cross-Sections by MATHCAD

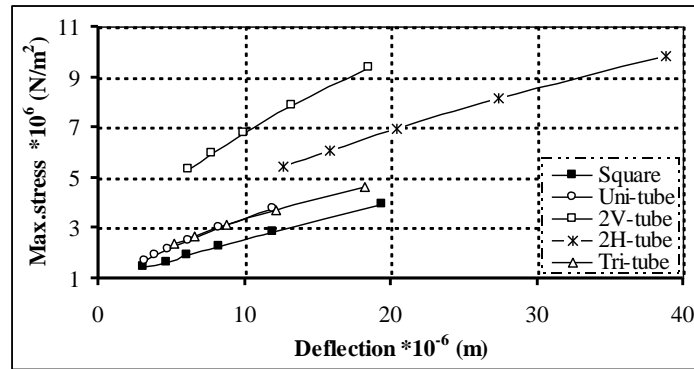


Fig. (24) Maximum Stress Versus Deflection in the Second Arm for Different Cross-Sections by MATHCAD

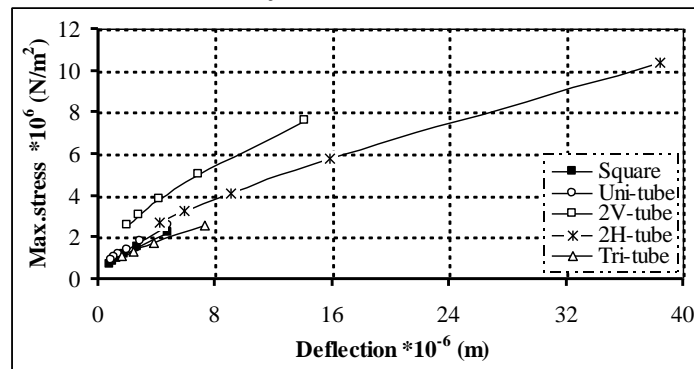


Fig. (25) Maximum Stress Versus Deflection in the Third Arm for Different Cross-Sections by MATHCAD

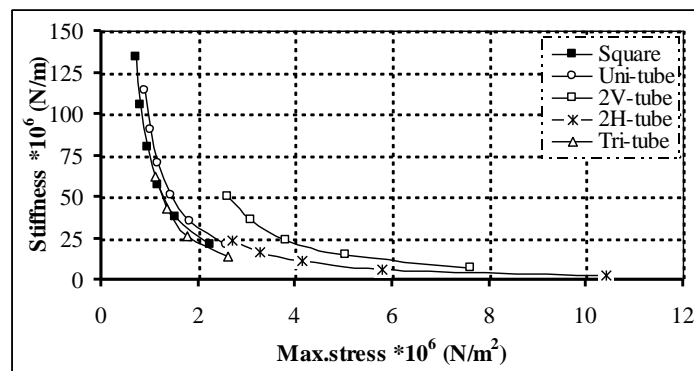


Fig. (26) Stiffness Versus Maximum Stress in the Third Arm for Different Cross-Sections by MATHCAD

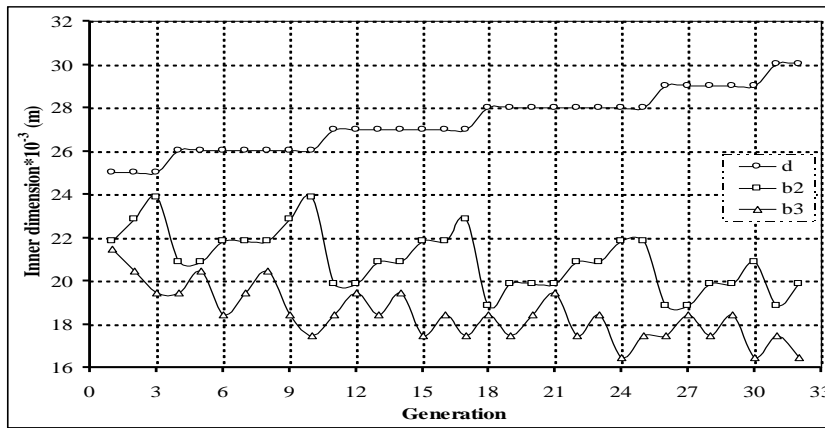


Fig. (27) Relation Between Inner Dimensions and Generation

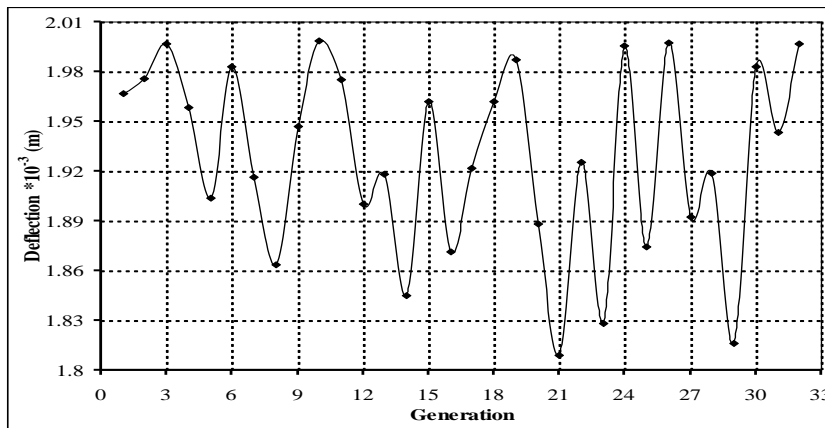


Fig. (28) Relation Between Total Deflection and Generation

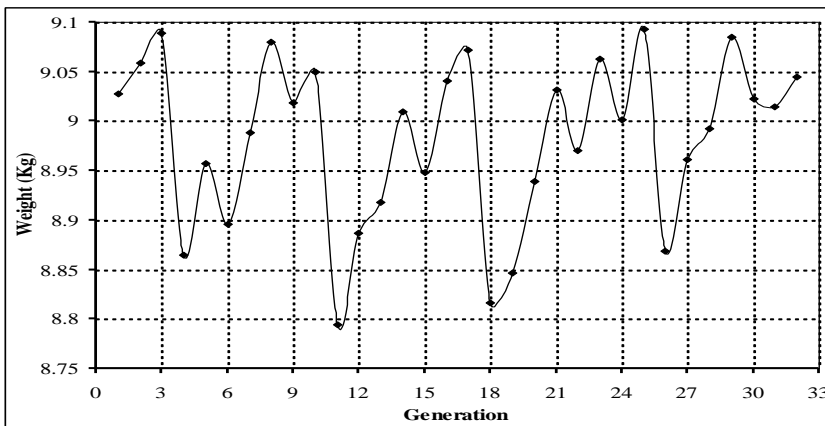


Fig. (29) Relation Between Total Weight and Generation

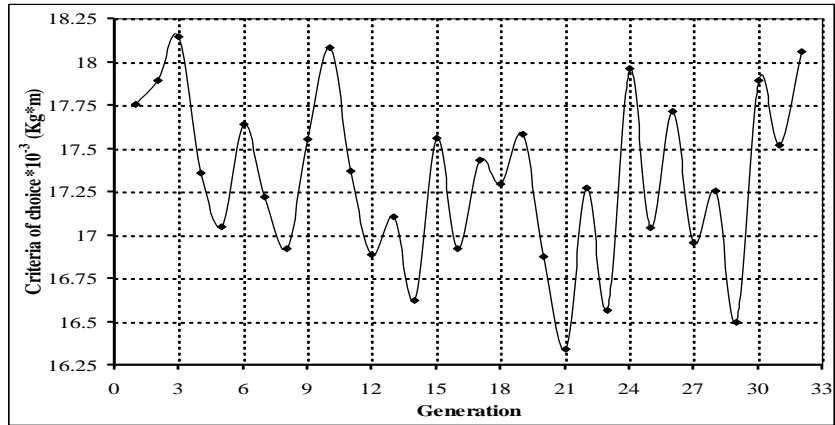


Fig. (30) Relation Between the Criteria of Choice and Generation

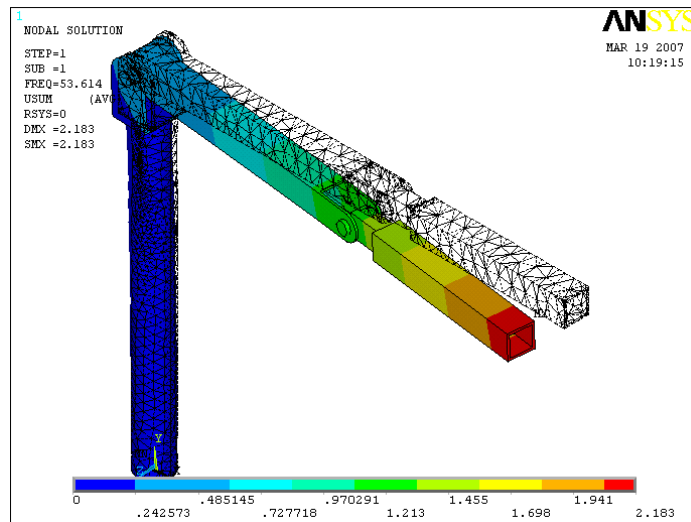


Fig. (31) First Mode Shape of Arms at (53.614Hz)

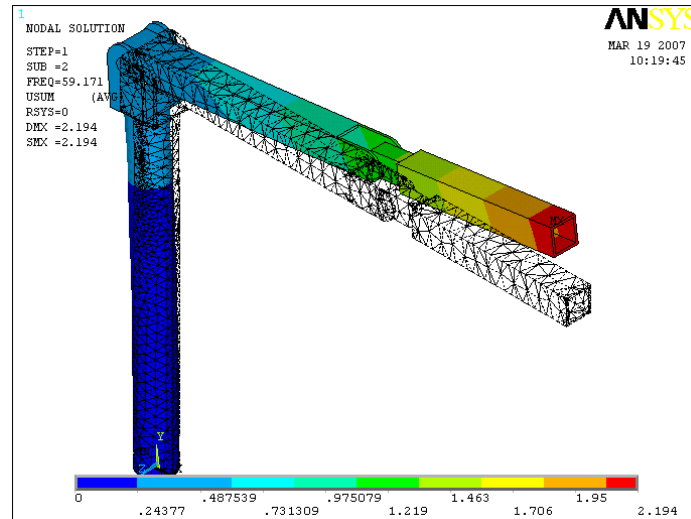
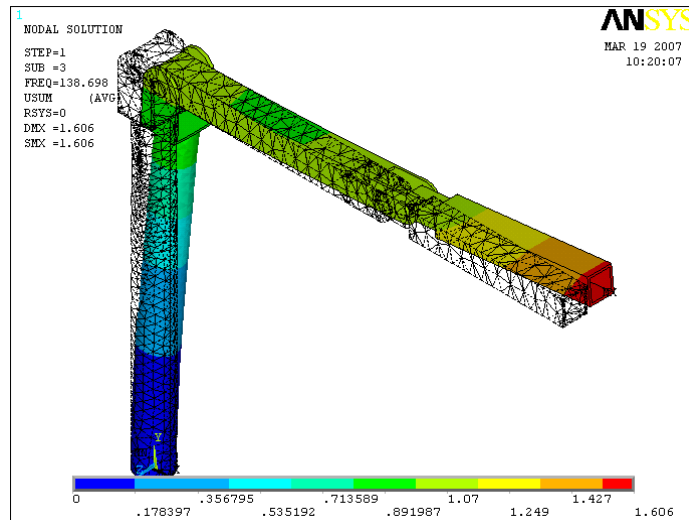


Fig. (32) Second Mode shape of Arms at (59.171Hz)



**Fig. (33) Third Mode Shape of Arms at (138.698Hz)**

## CONCLUSIONS

The main conclusions in our work (where we made a comparison between the five suggested sections for robot manipulator arms) is that to achieve best performance and high stiffness to weight ratio it is better to make the cross section of first arm as a circular tube and the other arms of the robot its better to make its section as a square tube.

Another perceptible notice is that the tri-tube section gives a results close to those of the uni-tube and square tube for the first, second and third arm respectively, the reason after this lag and retardation is that the stiffeners at the beginning and end of each arm takes parts of the metal or mass used in building or constructing the arms of the robot which make it weaker, this conclusion lead as to a results that the tri-tube section may gives a better results if an optimization had been made for it alone by varying the dimensions of the stiffness and the distance between the center's of the three tube and the diameter of each tube this may be as a suggestion for further work.

By the correct choice of cross section of each arm and by the appropriate choice of its dimensions based on the iteration and optimization process we may have a robot structure that has a weight, bigger by a little amount (about 25%) from the lightest weight which satisfies the condition of strength (i.e. the stress in each member reaches its maximum possible value) but satisfying the condition of stiffness which is the main feature of robot construction i.e. the error of the end effectors will be less than 2mm.

In case of increasing the weight or mass of the robot structure by an amount begin than 25% we can have a structure stiffer from the preceding and has deflection less than 0.002m but on the other hand we will sacrifices the benefit of low weight structure which minimizes the effect of inertia during the work of robot.

**REFERENCES**

- Abdel-Malek, K. and Paul, B. (1998). "Criteria for the Design of Manipulator Arms for a High Stiffness to Weight Ratio", *SME Journal of Manufacturing Systems*, Vol. 17, No. 3, P.P.209-220.
- Alazard, D.; Chretien, J. P. (1992). "The Impact of Local Masses and Inertias on the Dynamic Modeling of Flexible Manipulators".
- Ceccarelli, M.; Carobone, G. and Ottaviano, E. (2005). "Multi Criteria Optimum Design of Manipulators", *Bulletin technical sciences* Vol.53, No.1, P.P.9-18.
- Edward Mebarak. (2003). "On the Development of an Automated Design Procedure to Design Optimal Robots", Florida International University, Miami, Florida.
- Fresonke, D. A.; Hernandez, E. and Tesar, D. (1993). "Deflection Predictions for Serial Manipulators", in *IEEE Conference on Robotics and Automation*. Philadelphia, PA, pp482-487.
- Haubach, C. (2002) "Flexible Robots-an Example of Stochastic Structural Optimization". [www.stoch.net/daten/publical.htm#A](http://www.stoch.net/daten/publical.htm#A)
- Hearn, E. g. (1977). "Mechanics of Materials", Pergamon Press LTD.
- Henessey, M. P.; Priebe, J. A.; Paul, C. H. and Grommes, R. J. (2000) "Design of a Lightweight Robotic Arm and Controller," *IEEE Conference on Robotics and Automation*, Raleigh, NC. P.P.779-785.
- Jaydeep Roy and Louis, L. Whitcomb. (1999). "Comparative Structural Analysis of 2-DOF Semi-Direct-Drive Linkages for Robot Arms", *IEEE/ASME Transactions on Mechatronics*, Vol.4, No.1, pp.82-86.
- Leu, M. C.; Dukovski, V. and wang, K. K. (1985). "An Analytical and Experimental Study of the Stiffness of Robot Manipulators with Parallel Mechanism", *ASME Robotics and Manufacturing Automation*, Vol.15, P.P.137-143.
- Marcus Pettersson; Petter Krus; Xiaolong Feng; Johan Andersson and Daniel Wappling. (2004). "Industrial Robot Design Optimization in the Conceptual Design Phase". [http://www.machine.ikp.lin.se/staff/johan/files/IEEE\\_mecanic\\_and\\_robot\\_2004.pdf](http://www.machine.ikp.lin.se/staff/johan/files/IEEE_mecanic_and_robot_2004.pdf)
- Paredis, C. J. and Khosla, P. K. (1996). "Designing Fault-Tolerant Manipulators: How Many Degree of Freedom?", *Int. J. Rob. Res.*, Vol. 15, No. 6, P.P. 611-628.
- Rivin, E. I. (1988). "Mechanical Design of Robots", McGraw-Hill, Inc, Newyork.
- Saeed Moaveni. (1999). "Finite Element Analysis Theory and Application with ANSYS", Prentice-Hall.
- Shiakolas, P. S.; Koladiya, D. and Kebrle, J. (2002). "Optimum Robot Design Based on Task Specifications Using Evolutionary Techniques and Kinematic, Dynamic, and Structural Constraints", *International Journal of inverse problem in engineering*. Vol.10, No.4, P.P.359-375.

- Shimon. Y. Nof. (1999). “Handbook of Industrial Robotics”, John Wiley and Sons, Inc., Newyork.
- Williams, J. Angeles, and Bulca, F. (1993). “Design Philosophy of an Isotropic Six-Axis Serial Manipulator”, Robotics and Computer-Integrated Manufacturing, Vol.10, No.4, P.P.257-322.
- Wu, E. C.; Hwang, J. C. and Chladek, J. T. (1993). “Fault-Tolerant Joint Development for the Space Shuttle Remote Manipulator System: Analysis and Experiment”, IEEE Trans. Robot. Automat, Vol. 9, No. 5, P.P. 675-684.